International Journal of Control

ISSN: 0020-7179 (Print) 1366-5820 (Online) Journal homepage: https://www.tandfonline.com/loi/tcon20

UDE-based robust control for systems with mismatched uncertainties via feedback compensation

Zhen Tian, Qing-Chang Zhong, Beibei Ren & Jingqi Yuan

To cite this article: Zhen Tian, Qing-Chang Zhong, Beibei Ren & Jingqi Yuan (2019): UDE-based robust control for systems with mismatched uncertainties via feedback compensation, International Journal of Control, DOI: 10.1080/00207179.2019.1669826

To link to this article: https://doi.org/10.1080/00207179.2019.1669826

Published online: 26 Sep 2019.

INTERNATIONAL JOURNAL OF CONTROL
https://doi.org/10.1080/00207179.2019.1669826

Taylor & Francis
Taylor & Francis Group

UDE-based robust control for systems with mismatched uncertainties via feedback compensation

Zhen Tian[a,d], Qing-Chang Zhong[b], Beibei Ren[c] and Jingqi Yuan[d]

[a]School of Electrical Engineering and Automation, Wuhan University, Wuhan, People's Republic of China; [b]Department of Electrical and Computer Engineering, Illinois Institute of Technology, Chicago, IL, USA; [c]Department of Mechanical Engineering, Texas Tech University, Lubbock, TX, USA; [d]Department of Automation, Shanghai Jiao Tong University, Shanghai, People's Republic of China

ABSTRACT

The uncertainty and disturbance estimator (UDE)-based robust control is extensively investigated for its merits of strong robustness and straightforward principle. However, the structural constraint of UDE-based control limits its application to systems with matched uncertainties. In this paper, an improved UDE-based robust control strategy is proposed to address mismatched uncertainties so that it can be applied to systems with both matched and mismatched uncertainties. A modified reference model is designed with the feedback compensation of the estimated mismatched uncertainties. Besides, the estimated matched uncertainties are adopted for the feedforward control, as a compensation term of the robust control law. Moreover, the stability analysis and steady-state performance of the closed-loop system are presented. Simulations on a magnetic levitation system are carried out to illustrate the effectiveness and superiority of the proposed control scheme, which achieves robust stability and zero steady tracking error in the presence of both matched and mismatched uncertainties.

ARTICLE HISTORY
Received 6 September 2018
Accepted 5 September 2019

KEYWORDS
Uncertainty and disturbance estimator (UDE); robust control; mismatched uncertainties; modified reference model; feedback compensation

1. Introduction

Recently, the uncertainty and disturbance estimator (UDE)-based control approaches have been extensively investigated owing to its excellent performance and straightforward principle (Zhong, Kuperman, & Stobart, 2011; Zhong & Rees, 2004). The UDE-based robust control is widely applied to various-types systems, such as uncertain systems (Aharon, Shmilovitz, & Kuperman, 2018; Ren, Zhong, & Dai, 2017), time-delay systems (Sanz, Garcia, Albertos, & Zhong, 2017; Sun, Li, Zhong, & Lee, 2016) and nonlinear systems (Ren, Zhong, & Chen, 2015), where the time delay or nonlinearity is regarded as a disturbance-liked term. The core idea of the UDE-based robust control is that a continuous disturbance signal could be approximated in the frequency domain with proper filters. However, the previous studies on UDE-based controllers are only robust with respect to the matched uncertainties, which means the uncertainties and control inputs exist in the same channels. But for some practical systems, such as the permanent magnet synchronous machine (Liu & Li, 2012), the maglev suspension system (Cervera & Peretz, 2018; Yang, Zolotas, Chen, Michail, & Li, 2011) and power converters (Wang, Li, Yang, Wu, & Li, 2015), they are easily affected by mismatched uncertainties which may not satisfy the matched condition. For these systems with mismatched uncertainties, conventional UDE-based robust control approaches may fail to achieve satisfactory performance. In recent decades, some advanced control approaches have been studied to address the mismatched uncertainties, which are summarised as follows:

(1) Adaptive control methods. Adaptive mechanisms are embedded into the control law design so that the effects of mismatched uncertainties could be reduced. In Arefi, Jahed-Motlagh, and Karimi (2015), an adaptive neural network-based controller is designed for the stabilisation of nonlinear systems with mismatched uncertainties. An adaptive fuzzy robust control method with the integration of H_∞ and backstepping control techniques is developed for uncertain nonlinear systems (Zhai, An, Dong, & Zhang, 2017). An adaptive robust stabilisation approach is proposed for nonlinear systems to overcome the effects of mismatched time-varying parameters (Arefi & Jahed-Motlagh, 2012). An adaptive controller based on time-varying sliding-mode function is proposed to handle the mismatched uncertainties with unknown upper bounds (Zhang, Shi, & Xia, 2010; Zhu & Zhu, 2014). However, these adaptive control methods may be conservative to be applied because there are several assumptions on the structure of the nominal system and mismatched uncertainties.

(2) Observer-based control methods. Based on the feedforward control principle, some observer-based control approaches have been investigated to deal with the mismatched uncertainties. With a proper disturbance compensation gain, a composite controller is proposed to address the mismatched disturbances (Yang et al., 2011). A disturbance observer-based

CONTACT Qing-Chang Zhong zhongqc@ieee.org Department of Electrical and Computer Engineering, Illinois Institute of Technology, Chicago, IL 60616 USA

controller (DOBC) is proposed for the air-breathing hypersonic vehicles (An, Liu, Wang, & Wu, 2016), integrated with feedback linearisation method. Similarly, an extended state observer (ESO)-based controller is designed for rotor-active magnetic bearings (AMBs) systems with mismatched uncertainties (Liu, Liu, & Fang, 2017). Besides, the active disturbance rejection control (ADRC) approach is proposed based on the ESO to counteract the mismatched uncertainties (Guo & Wu, 2017). A generalised ESO-based approach is proposed for nonintegral-chain systems subject to mismatched uncertainties (Li, Yang, Chen, & Chen, 2012). A nonlinear ESO-based controller is constructed for multi-input-multi-output systems to achieve robust tracking (Zhao & Guo, 2018). However, for these observer-based approaches, the first derivatives of the mismatched uncertainties are assumed to be bounded and converge to zero at the steady state, which is hardly guaranteed in practice since the mismatched uncertainties are generally unknown and time-varying. Moreover, the parameters tuning becomes much more complicated for high-order observers.

(3) Sliding-mode control (SMC) methods. The function approximation technique is adopted to decompose the mismatched uncertainties into several orthonormal basis functions, which enables a multiple surface sliding-mode control law (Huang & Chen, 2004). A nonlinear integral-type sliding-mode surface and a virtual nonlinear nominal control law are integrated to address both the matched and mismatched uncertainties (Cao & Xu, 2004). Such an integral variable structure controller is also applied to the flexible spacecraft with mismatched uncertainties (Hu, 2007). A linear matrix inequality (LMI)-based sliding surface is designed to render an integral sliding-mode controller for mismatched uncertain systems (Andrade-Da Silva, Edwards, & Spurgeon, 2009). A finite-time disturbance observer-based terminal sliding-mode control approach is proposed (Wang, Li, Yang, Wu, & Li, 2016), which exhibits good nominal performance recovery as well as chattering alleviation. A nonlinear disturbance observer is designed for the estimation of mismatched uncertainties (Yang, Li, & Yu, 2013), which enables a robust control law to the mismatched uncertainties. Similarly, an extended disturbance observer is applied to counteract the mismatched uncertainties (Ginoya, Shendge, & Phadke, 2014). Nevertheless, these SMC methods need to know the upper bound of the mismatched uncertainties, which is difficult to be obtained due to the complexity of practical control plants and disturbances. Besides, the well-known chattering phenomenon has become an obstacle for the applications of sliding-mode control approaches.

(4) Other methods. A UDE-based backstepping control method is proposed for nonlinear systems with mismatched uncertainties, which addresses the 'complexity explosion' problem in conventional backstepping approach (Dai, Ren, & Zhong, 2016, 2018). A UDE-based adaptive sliding-mode control method is presented for nonlinear systems with parameter uncertainties (Londhe, Dhadekar, Patre, & Waghmare, 2017), where a nonlinear observer and the UDE are applied to the estimation of the mismatched and matched uncertainties, respectively.

In this paper, an improved UDE-based robust control approach is proposed to address the mismatched uncertainties, which relaxes the structural constraints on the nominal systems and disturbances that have appeared in previous studies. Both the matched and mismatched uncertainties are estimated by the UDE, where only the spectrum of the lumped uncertainties is required. The matched uncertainty is compensated by feedforward control while the mismatched uncertainty is introduced into the feedback control loop, which maintains fast response of the feedforward control. Moreover, the internal model principle is adopted for the controller and UDE design, which guarantees the asymptotic reference tracking and disturbance rejection.

The rest of this paper is organised as follows. In Section 2, the limitations of conventional UDE-based control approach are presented. Design details of the UDE-based robust controller for systems with mismatched uncertainties are given in Sections 3 to 5, including the controller design, UDE-filter design and reference system design. Section 6 gives the proof of the closed-loop stability and steady-state tracking performance. To illustrate the effectiveness of the proposed control approach, simulation results on a magnetic levitation system are presented in Section 7. Concluding remarks are summarised in Section 8.

2. Overview of the UDE-based robust control

Consider the following uncertain linear time-invariant system:

$$\begin{cases} \dot{x} = (A + \Delta A)\, x + Bu + d \\ y = Cx \end{cases} \tag{1}$$

where $x \in R^n$ is the system state, $u \in R$ is the control input, $y \in R$ is the system output; $A \in R^{n\times n}$ denotes the known system matrix, $B \in R^{n\times 1}$ denotes the control matrix, $C \in R^{1\times n}$ denotes the output matrix; $\Delta A \in R^{n\times n}$ denotes the model uncertainties and $d \in R^{n\times 1}$ denotes the unknown external disturbances. Since this paper mainly focuses on dealing with the mismatched uncertainties, the uncertainty on control matrix B is not considered. If the uncertainty on the control matrix B is bounded in a relative small domain and satisfies the matching conditions (see Assumption 5 in Dai et al. (2018)), the proposed UDE-based control approach still works. More details about how to handle the control matrix uncertainty are available in Dai et al. (2018).

The lumped uncertainty u_d is represented as

$$u_d = \Delta A \cdot x + d.$$

In general, the uncertainty is called the matched term if it acts on the same channels as the control input. Otherwise, it is called the mismatched uncertainty. Therefore, the lumped uncertain term u_d could be decomposed as two components, i.e. the matched term u_{dm} and the mismatched term u_{dmis}, such that

$$\begin{aligned} u_d &= BB^{+}u_d + \left(I - BB^{+}\right) u_d \\ &= u_{dm} + u_{dmis}, \end{aligned}$$

where $B^{+} = (B^TB)^{-1}B^T$ denotes the pseudo inverse of B. The matched component is $u_{dm} = BB^{+}u_d$ and the mismatched component is $u_{dmis} = (I - BB^{+})u_d$.

Without loss of generality, the pair $(A,\ B)$ is assumed controllable. The control objective is to design a robust control law such that the system output y could accurately track the given reference signal $r \in R$ in the presence of model uncertainties

and disturbances. To facilitate the controller design, a reference model is introduced as following:

$$\begin{cases} \dot{x}_m = A_m x_m + B_m u_m \\ y_m = C_m x_m \end{cases} \tag{2}$$

where $x_m \in R^n$ is the reference model state, $u_m \in R$ is the reference model input, $y_m \in R$ is the reference model output; $A_m \in R^{n\times n}$, $B_m \in R^{n\times 1}$ and $C_m \in R^{1\times n}$ denote the system matrix, input matrix and output matrix of the reference model, respectively. The reference model is determined by the desired performance of the closed-loop system. Thus, the system (1) could achieve good performance if system states x are driven to track the reference model states x_m. Define the tracking error

$$e = x_m - x,$$

which is expected to satisfy the desired dynamics as follows:

$$\dot{e} = (A_m + K)\, e, \tag{3}$$

where $K \in R^{n\times n}$ is a feedback gain such that $A_m + K$ is Huriwtz.

Substituting Equations (1) and (2) into Equation (3), one yields

$$Bu = (A_m - A)\, x + B_m u_m - Ke - u_d. \tag{4}$$

Then the control law is obtained,

$$u = B^+ \left[(A_m - A)\, x + B_m u_m - Ke - u_d\right]. \tag{5}$$

To implement the control law, an uncertainty and disturbance estimator is designed for the estimation of the unknown term u_d in Equation (5). According to [2], u_d is estimated as follows:

$$\hat{u}_d = (\dot{x} - Ax - Bu) \star g_f(t), \tag{6}$$

where '$\star$' denotes the conventional convolution operator and $g_f(t)$ denotes the impulse response of a frequency-selective filter with unity gain and zero phase shift, covering the spectrum of u_d. By replacing u_d by $\hat{u}_d$ in Equation (5), the UDE-based control law is

$$u = B^+ \left[(A_m - A)\, x + B_m u_m - Ke - \hat{u}_d\right]. \tag{7}$$

By substituting Equation (6) into Equation (7), the general representation of the UDE-based control law (7) in the time domain is

$$u = B^+ \left\{ -Ax + \mathcal{L}^{-1}\left[\frac{1}{1 - G_f(s)}\right] \star (A_m x + B_m u_m - Ke) - \mathcal{L}^{-1}\left[\frac{sG_f(s)}{1 - G_f(s)}\right] \star x \right\}, \tag{8}$$

where $G_f(s)$ is the Laplace transform of $g_f(t)$ and $\mathcal{L}^{-1}[\cdot]$ denotes the inverse Laplace transform operator.

To guarantee zero steady tracking error, the following structural constraint should be satisfied (Ren et al., 2017):

$$\left(I - BB^+\right)\left[A_m x + B_m u_m - Ax - u_d - Ke\right] = 0, \tag{9}$$

which implies the structural constraint on the mismatched uncertainty represented as follows:

$$\begin{aligned} u_{dmis} &= \left(I - BB^+\right) u_d \\ &= \left(I - BB^+\right)\left[A_m x + B_m u_m - Ax - Ke\right]. \end{aligned} \tag{10}$$

Considering that the mismatched uncertainty u_{dmis} is generally unknown and time-varying, the condition (10) is hard to be satisfied. That is to say, the conventional UDE-based robust controller (8) is sensitive to the mismatched uncertainty.

3. Improved design of the UDE-based controller

The UDE-based robust control scheme proposed in this paper is summarised in Figure 1, which is composed of four loops. The first loop is the reference model control loop, where the internal model principle is embedded to achieve asymptotic tracking of the reference signal r. The second loop is the tracking error feedback control loop, which is applied to drive the system states to track the reference model states. The third loop is the feedforward control loop to achieve the matched uncertainties compensation, where the UDE is adopted for the estimation of uncertainties and disturbances. The last loop is the feedback compensation loop to eliminate the effects of the mismatched uncertainties. It is worth noting that the reference tracking, matched disturbance rejection and mismatched uncertainty compensation are decoupled in the frequency domain, which is the so-called three-degree-of-freedom nature.

To address the mismatched uncertainties, a modified reference model with the compensation of the estimated mismatched uncertainties is designed as follows:

$$\begin{cases} \dot{x}_m = A_m x_m + B_m u_m + \hat{u}_{dmis} \\ y_m = C_m x_m \end{cases} \tag{11}$$

where $\hat{u}_{dmis} = (I - BB^+)\hat{u}_d$ is derived from the estimation of UDE denoted as Equation (6). Correspondingly, the control law is designed as

$$u = B^+ \left[(A_m - A)\, x + B_m u_m + \hat{u}_{dmis} - Ke - \hat{u}_d\right]. \tag{12}$$

By substituting Equation (6) into Equation (12), the UDE-based control law is formulated in the time domain as follows:

$$u = B^+ \left\{ -\mathcal{L}^{-1}\left[\frac{I - BB^+ G_f(s)}{1 - G_f(s)}\right] \star (Ax) + \mathcal{L}^{-1}\left[\frac{1}{1 - G_f(s)}\right] \star (A_m x + B_m u_m - Ke) - \mathcal{L}^{-1}\left[\frac{sG_f(s)}{1 - G_f(s)}\right] \star \left(BB^+ x\right) \right\} \tag{13}$$

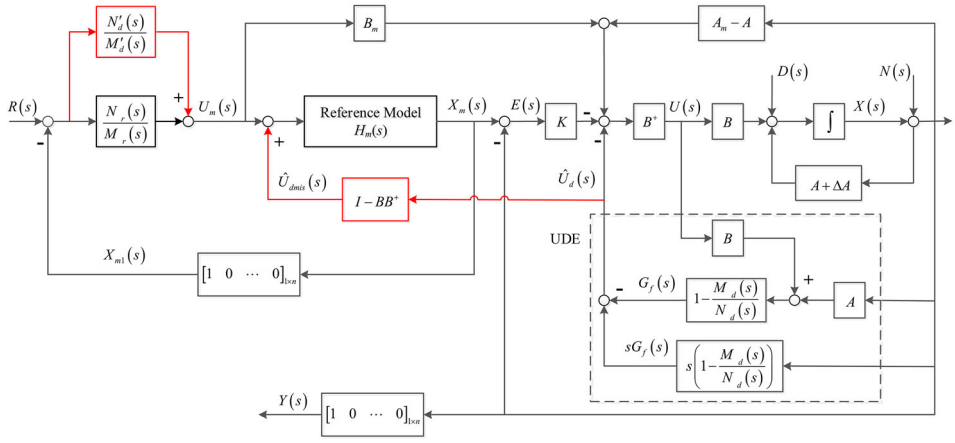

Figure 1. Block diagram of the proposed UDE-based robust control scheme.

4. The filter design

The fundamental constraint for the filter $G_f(s)$ is that its bandwidth should be wide enough to cover the spectrum of u_d. In general, $G_f(s)$ is selected as a low-pass filter,

$$G_f(s) = 1 - \frac{M_d(s)}{N_d(s)}, \tag{14}$$

where $N_d(s)$ and $M_d(s)$ are appropriate polynomial functions of s such that $G_f(s)$ maintains stable and $\frac{M_d(\infty)}{N_d(\infty)}$ is finite. $M_d(s)$ could be determined by the exosystem model of the disturbance signal d, which is represented as follows (Ren et al., 2017):

$$\begin{aligned} \dot{w}_d(t) &= S_d w_d(t), \\ d(t) &= P_d w_d(t), \end{aligned} \tag{15}$$

where $w_d(t)$ is the state of the exosystem model of the disturbance signal $d(t)$, S_d and P_d are the feature matrices of $d(t)$. Then, $M_d(s)$ could be chosen as the characteristic function of S_d, *i.e.*,

$$M_d(s) = |sI - S_d|. \tag{16}$$

More details about the filter design for different-type signals are available in the literature (Ren et al., 2017). It is worth noticeable that the upper bound of the disturbance signal is not necessarily known and only the frequency information (bandwidth) is required for the UDE-filter design. Compared with the magnitude, the frequency information of the signal is more likely to be available (Marino & Tomei, 2014).

5. Reference system design

According to the well-known internal model principle (Francis & Wonham, 1976), the asymptotic reference tracking or disturbance rejection could be achieved if the exosystem that is to generate the reference trajectory or the disturbance is introduced into the feedback mechanism. In order to simultaneously achieve the reference tracking and mismatched disturbance rejection, the control scheme shown in the left part of Figure 1 is designed to generate the reference command $u_m(t)$ such that the reference model output $x_{m1}(t)$ could asymptotically track the reference signal $r(t)$.

For the closed-loop system shown in Figure 1, the reference system output $X_{m1}(s)$ could be represented as follows:

$$\begin{aligned} X_{m1}(s) = H_{m_1}(s) \cdot \left[\frac{N_r(s)}{M_r(s)} + \frac{N'_d(s)}{M'_d(s)}\right] \\ \cdot [R(s) - X_{m1}(s)] + H_{m_1}(s) \cdot \hat{U}_{dmis}(s), \end{aligned} \tag{17}$$

where $\frac{N_r(s)}{M_r(s)}$ and $\frac{N'_d(s)}{M'_d(s)}$ are two parallel controllers based on the exosystem models of the reference signal $R(s)$ and mismatch uncertainty $\hat{U}_{dmis}(s)$, respectively; $H_m(s)$ denotes the transfer function of the reference model, and $H_{m_1}(s) = [1\ 0, \cdots\ 0]_{1\times n} \cdot H_m(s)$.

According to Equation (6), the estimated mismatched uncertainties $\hat{U}_{dmis}(s)$ is represented as

$$\begin{aligned} \hat{U}_{dmis}(s) &= \left(I - BB^+\right) U_d(s) G_f(s) \\ &= \left(I - BB^+\right) [\triangle A \cdot X(s) + D(s)] G_f(s), \end{aligned} \tag{18}$$

where $X(s)$, $D(s)$ and $G_f(s)$ denote the Laplace transform of $x(t)$, $d(t)$ and $g_f(t)$, respectively.

If the closed-loop system is designed stable (illustrated in Section 6), there must exist a stable transfer function $G_{RX}(s)$ from the reference signal $R(s)$ to the system state $X(s)$ such that

$$X(s) = G_{RX}(s) R(s). \tag{19}$$

Substituting Equations (18) and Equation (19) into Equation (17), the transfer function from $R(s)$ to $X_{m1}(s)$ is acquired,

$$\begin{aligned} \frac{X_{m1}(s)}{R(s)} = &\frac{\left[N_r(s) M'_d(s) + M_r(s) N'_d(s)\right] H_{m_1}(s)}{M_r(s) M'_d(s) + \left[N_r(s) M'_d(s) + M_r(s) N'_d(s)\right] H_{m_1}(s)} \\ &+ \frac{M_r(s) M'_d(s) H_{m_1}(s) \left(I - BB^+\right) \triangle A \cdot G_{RX}(s) G_f(s)}{M_r(s) M'_d(s) + \left[N_r(s) M'_d(s) + M_r(s) N'_d(s)\right] H_{m_1}(s)}. \end{aligned} \tag{20}$$

Since $M_r(s)$ in Equation (20) is selected such that $M_r(s) = 0$ at the modes of the reference signal $r(t)$, the steady-state gain

equals to one, which guarantees the asymptotic tracking of the closed-loop system. That is to say, $X_{m1}(s) \to r(t)$ when $t \to \infty$.

According to Equation (17) and (18), the transfer function from $D(s)$ to $X_{m1}(s)$ is represented as follows:

$$\frac{X_{m1}(s)}{D(s)} = \frac{M_r(s) M_d'(s) H_{m_1}(s) \left(I - BB^+\right) G_f(s)}{M_r(s) M_d'(s) + \left[N_r(s) M_d'(s) + M_r(s) N_d'(s)\right] H_{m_1}(s)} \tag{21}$$

Since $M_d'(s)$ in Equation (21) is selected such that $M_d'(s) = 0$ at the modes of the mismatched disturbance $u_{dmis}(t)$, the steady-state gain equals to zero, which guarantees the disturbance rejection of the closed-loop system. That is to say, the mismatched disturbance $d(t)$ has no impact on $X_{m1}(s)$ when $t \to \infty$. Three special cases are presented below.

5.1 Tracking a step signal in the presence of step mismatched disturbance

If the reference signal and disturbance signal are both step signals, according to the internal model principle, there is

$$M_r(s) = s,$$
$$M_d'(s) = s.$$

Then $N_r(s)$ and $N_d'(s)$ could be selected as

$$N_r(s) = a_1 s + a_2,$$
$$N_d'(s) = b_1 s + b_2,$$

with the parameters $a_1,\ a_2 > 0$ and $b_1,\ b_2 > 0$, which could be easily designed by pole assignment approach. Based on Equation (17), at $s = 0$, there are

$$\begin{aligned}\frac{X_{m1}(0)}{R(0)} &= \lim_{s\to 0} \frac{X_{m1}(s)}{R(s)} \\ &= \frac{(a_2 + b_2) H_{m_1}(0)}{(a_2 + b_2) H_{m_1}(0)} + 0 \\ &= 1\end{aligned}$$

and

$$\begin{aligned}\frac{X_{m1}(0)}{D(0)} &= \lim_{s\to 0} \frac{X_{m1}(s)}{D(s)} \\ &= \frac{0 \cdot H_{m_1}(0) \left(I - BB^+\right) G_f(0)}{(a_2 + b_2) H_{m_1}(0)} \\ &= 0,\end{aligned}$$

which simultaneously guarantees the asymptotic tracking of a step reference and the disturbance rejection of a step disturbance.

5.2 Tracking a sinusoidal signal in the presence of sinusoidal mismatched disturbance

For a sinusoidal reference signal with the known frequency ω_r and a sinusoidal disturbance signal with the known frequency ω_d, according to the internal model principle, there is

$$M_r(s) = s^2 + \omega_r^2,$$
$$M_d'(s) = s^2 + \omega_d^2,$$

$N_r(s)$ and $N_d'(s)$ are chosen as

$$N_r(s) = a_1 s + a_2,$$
$$N_d'(s) = b_1 s + b_2,$$

with $a_1,\ a_2 > 0$ and $b_1,\ b_2 > 0$. Based on Equation (20), at the frequency ω_r, there is

$$\begin{aligned}\frac{X_{m1}(j\omega_r)}{R(j\omega_r)} &= \lim_{s\to j\omega_r} \frac{X_{m1}(s)}{R(s)} \\ &= \frac{\left(\omega_d^2 - \omega_r^2\right)\left(j \cdot a_1\omega_r + a_2\right) H_{m_1}(j\omega_r)}{\left(\omega_d^2 - \omega_r^2\right)\left(j \cdot a_1\omega_r + a_2\right) H_{m_1}(j\omega_r)} + 0 \\ &= 1.\end{aligned}$$

Based on Equation (21), at the frequency ω_d, there is

$$\begin{aligned}\frac{X_{m1}(j\omega_d)}{D(j\omega_d)} &= \lim_{s\to j\omega_d} \frac{X_{m1}(s)}{D(s)} \\ &= \frac{0 \cdot H_{m_1}(j\omega_d)\left(I - BB^+\right) G_f(j\omega_d)}{\left(\omega_r^2 - \omega_d^2\right)\left(j \cdot b_1\omega_d + b_2\right) H_{m_1}(j\omega_d)} \\ &= 0,\end{aligned}$$

which indicates the asymptotic tracking of a sinusoidal reference and the disturbance rejection of a sinusoidal disturbance.

5.3 Tracking a step signal in the presence of sinusoidal mismatched disturbance

If the reference signal is a step signal and the disturbance is a sinusoidal signal with the known frequency ω_d, according to the internal model principle, there is

$$M_r(s) = s,$$
$$M_d'(s) = s^2 + \omega_d^2,$$

$N_r(s)$ and $N_d'(s)$ are selected as

$$N_r(s) = a_1 s + a_2,$$
$$N_d'(s) = b_1 s + b_2$$

with $a_1,\ a_2 > 0$ and $b_1,\ b_2 > 0$. Based on Equation (20), at $s = 0$, there is

$$\begin{aligned}\frac{X_{m1}(0)}{R(0)} &= \lim_{s\to 0} \frac{X_{m1}(s)}{R(s)} \\ &= \frac{\left(a_2\omega_d^2 + b_2\right) H_{m_1}(0)}{\left(a_2\omega_d^2 + b_2\right) H_{m_1}(0)} + 0 \\ &= 1.\end{aligned}$$

Based on Equation (21), at the frequency ω_d, there is

$$\begin{aligned}\frac{X_{m1}\left(j\omega_d\right)}{D\left(j\omega_d\right)} &= \lim_{s\to j\omega_d}\frac{X_{m1}(s)}{D(s)}\\ &= \frac{0\cdot H_{m_1}\left(j\omega_d\right)\left(I-BB^{+}\right)G_f\left(j\omega_d\right)}{j\omega_d\cdot\left(j\cdot b_1\omega_d+b_2\right)H_{m_1}\left(j\omega_d\right)}\\ &= 0,\end{aligned}$$

which implies the closed-loop system achieves the asymptotic tracking of a step reference and the disturbance rejection of a sinusoidal disturbance.

6. Stability and robustness analysis

6.1 Closed-loop stability

Taking the time derivative of e based on Equations (1), (11) and (12), there is

$$\begin{aligned}\dot{e} &= A_m x_m + B_m u_m + \left(I-BB^{+}\right)\hat{u}_d - u_d\\ &\quad -\left[A+BB^{+}\left(A_m-A\right)\right]x - BB^{+}\left(B_m u_m - Ke - \hat{u}_d\right)\\ &= \left[A_m+K-\left(I-BB^{+}\right)\left(A_m+K-A\right)\right]e\\ &\quad +\left(I-BB^{+}\right)\cdot\left[\left(A_m-A\right)x_m+B_m u_m\right]+\tilde{u}_d,\end{aligned}\tag{22}$$

where $\tilde{u}_d = u_d - \hat{u}_d$ denotes the estimation error of the lumped uncertainty. The closed-loop system matrix in Equation (22) is denoted as

$$A_c = A_m + K - \left(I-BB^{+}\right)\left(A_m+K-A\right).$$

Based on Equations (11) and (12), the closed-loop dynamics of x is represented as

$$\dot{x} = A_c x + BB^{+}\left(B_m u_m - Kx_m\right) + \tilde{u}_d\tag{23}$$

According to Equation (6) and the definition of u_d, the Laplace transform of $\tilde{u}_d$ is

$$\tilde{U}_d(s) = \left(\triangle A\cdot X(s) + D(s)\right)\left(1-G_f(s)\right).\tag{24}$$

Taking the Laplace transform of Equation (23) and substituting Equation (24) into it, there is

$$\begin{aligned}&\left[sI-A_c-\left(1-G_f(s)\right)\cdot\triangle A\right]X(s)\\ &\quad = BB^{+}\left(B_m U_m(s) - KX_m(s)\right)\\ &\qquad +\left(1-G_f(s)\right)D(s).\end{aligned}\tag{25}$$

The closed-loop dynamics is

$$\begin{aligned}&\left[I-(sI-A_c)^{-1}\cdot\triangle A\cdot\left(1-G_f(s)\right)\right]X(s)\\ &\quad = (sI-A_c)^{-1}\left\{BB^{+}\left(B_m U_m(s) - KX_m(s)\right)\right.\\ &\qquad \left.+\left(1-G_f(s)\right)D(s)\right\}.\end{aligned}\tag{26}$$

The equivalent block diagram of the closed-loop system represented in Equation (26) is shown in Figure 2, where the equivalent input is

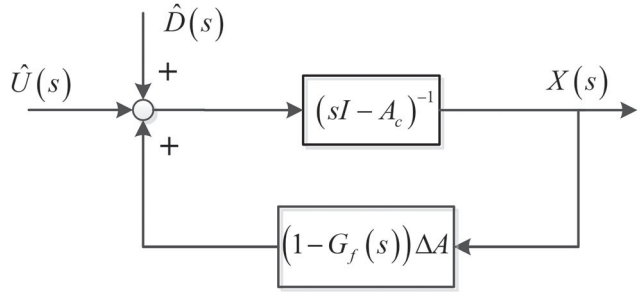

Figure 2. Equivalent block diagram of the closed-loop system represented as Equation (26).

$$\hat{U}(s) = BB^{+}\left(B_m U_m(s) - KX_m(s)\right)$$

and the equivalent external disturbance is

$$\hat{D}(s) = \left(1-G_f(s)\right)D(s).$$

The term $(sI-A_c)^{-1}$ denotes the transfer function of the nominal system and the term $(1-G_f(s))\cdot\triangle A$ denotes the feedback loop gain.

Theorem 6.1: *Assume that the 2-norm of uncertain matrix satisfies $\|\triangle A\|\le\gamma$, where γ is a known positive scalar. The uncertain linear system* (1) *with the UDE-based control law* (12) *is bounded-input bounded-output (BIBO) stable if the following conditions are satisfied:*

(a) *A_m is Hurwitz;*
(b) *A_c is Hurwitz;*
(c) *The stable filter $G_f(s)$ is designed to meet*

$$\left\|(sI-A_c)^{-1}\left(1-G_f(s)\right)\right\|_\infty < \frac{1}{\gamma}$$

Proof: If the above conditions are satisfied, the following inequation holds:

$$\left\|(sI-A_c)^{-1}\left(1-G_f(s)\right)\cdot\triangle A\right\|_\infty < \frac{1}{\gamma}\cdot\gamma = 1.\tag{27}$$

According to Equation (26) and the small-gain theorem (Khalil, 1996), the closed-loop system is BIBO stable. ■

Since appropriate A_m is designed to guarantee the stability of the reference model control loop, the reference state x_m and input u_m are both bounded. Assuming that the external disturbance $D(s)$ is bounded, then the term $(I-BB^{+})\cdot[(A_m-A)x_m+B_m u_m]+\tilde{u}_d$ in Equation (22) is bounded. Since the closed-loop system (22) is BIBO stable, the tracking error e is bounded.

6.2 Steady-state performance

The following theorem is presented to illustrate the proposed method could achieve zero steady tracking error in the presence of uncertainties and disturbances.

Theorem 6.2: *Assume that the system shown in Figure 1 satisfies the following structural constraints:*

$$\begin{aligned}\left(I-BB^{+}\right)\left(A_m-A\right)&=0,\\ \left(I-BB^{+}\right)B_m&=0.\end{aligned}\tag{28}$$

If the closed-loop system (26) is stable, and the filter $G_f(s)$ is designed to meet the following conditions:

$$\begin{aligned}\lim_{s\to 0}s\left(1-G_f\left(s\right)\right)\cdot R\left(s\right)&=0\\ \lim_{s\to 0}s\left(1-G_f\left(s\right)\right)\cdot D\left(s\right)&=0\end{aligned}\tag{29}$$

then the closed-loop system achieves zero steady-state tracking error.

Proof: Taking the Laplace transform of Equation (22),

$$\begin{aligned}E\left(s\right)=\left(sI-A_c\right)^{-1}\{&\left(I-BB^{+}\right)\cdot\left[\left(A_m-A\right)X_m\left(s\right)\right.\\ &\left.+B_mU_m\left(s\right)\right]+BB^{+}\tilde{U}_d\left(s\right)\},\end{aligned}\tag{30}$$

where $E(s)$, $X_m(s)$, $U_m(s)$, $U_d(s)$ and $\tilde{U}_d(s)$ denote the Laplace transform of $e(t)$, $x_m(t)$, $u_m(t)$, $u_d(t)$ and $\tilde{u}_d(t)$, respectively.

According to Equation (28), there is

$$\left(I-BB^{+}\right)\left[\left(A_m-A\right)X_m\left(s\right)+B_mU_m\left(s\right)\right]=0.\tag{31}$$

Thus, $E(s)$ is simplified as

$$\begin{aligned}E\left(s\right)&=\left(sI-A_c\right)^{-1}BB^{+}\tilde{U}_d\left(s\right)\\ &=\left(sI-A_c\right)^{-1}BB^{+}U_d\left(s\right)\left(1-G_f\left(s\right)\right).\end{aligned}\tag{32}$$

Since the closed-loop system (26) is designed stable, Equation (18) holds. And if the condition (29) is satisfied,there is

$$\begin{aligned}&\lim_{s\to 0}s\left(1-G_f\left(s\right)\right)U_d\left(s\right)\\ &=\lim_{s\to 0}s\left(1-G_f\left(s\right)\right)\left[\triangle A\cdot G_{RX}\left(s\right)R\left(s\right)+D\left(s\right)\right]\\ &=\lim_{s\to 0}\triangle A\cdot G_{RX}\left(s\right)\cdot s\left(1-G_f\left(s\right)\right)R\left(s\right)\\ &\quad+\lim_{s\to 0}s\left(1-G_f\left(s\right)\right)D\left(s\right)\\ &=0.\end{aligned}\tag{33}$$

According to the final value theorem, there is

$$\begin{aligned}\lim_{t\to\infty}e\left(t\right)&=\lim_{s\to 0}sE\left(s\right)\\ &=\lim_{s\to 0}\left(sI-A_c\right)^{-1}BB^{+}\cdot s\left(1-G_f\left(s\right)\right)U_d\left(s\right)\\ &=0.\end{aligned}$$

Therefore, the closed-loop system achieves zero steady-state tracking error. ■

In Theorem 6.2, the conditions in Equation (29) could be satisfied while appropriate filter $G_f(s)$ is selected. The internal model principle could be adopted for the design of $G_f(s)$ to achieve asymptotic reference tracking and disturbance rejection (Ren et al., 2017).

7. Application to a magnetic levitation system

7.1 System description

The schematic diagram of a MagLev system is displayed in Figure 3. The system is controlled by the voltage u, which introduces a current i in the electromagnet to build a magnetic field. The ball position q can be regulated by changing the voltage amplitude. The linearised state-space model of a MagLev system is represented as follows (Goodall, Michail, Whidborne, & Zolotas, 2009):

$$\begin{cases}\dot{x}=Ax+Bu+\triangle A\cdot x+d\\ y=Cx\end{cases}\tag{34}$$

where $x=[\,q\ \dot{q}\ i\,]^{\mathrm{T}}$ is the system state, u is the control input (voltage) and $y=q$ is the system output; $\triangle A$ and d denote the model uncertainties and external disturbances, respectively, and let $u_d=\triangle A\cdot x+d$ denote the general uncertainties and disturbances; A, B and C denotes the system matrix, input matrix and output matrix, respectively, which are represented as

$$A=\begin{bmatrix}0 & 1 & 0\\ 2K_f\dfrac{I_o^2}{M_sG_o^3} & 0 & -2K_f\dfrac{I_o}{M_sG_o}\\ 0 & 0 & \dfrac{-R_c}{L_c+K_bN_cA_p/G_o}\end{bmatrix}$$

$$B=\begin{bmatrix}0 & 0 & \dfrac{1}{L_c+K_bN_cA_p/G_o}\end{bmatrix}^{\mathrm{T}}$$

$$C=\begin{bmatrix}1 & 0 & 0\end{bmatrix}$$

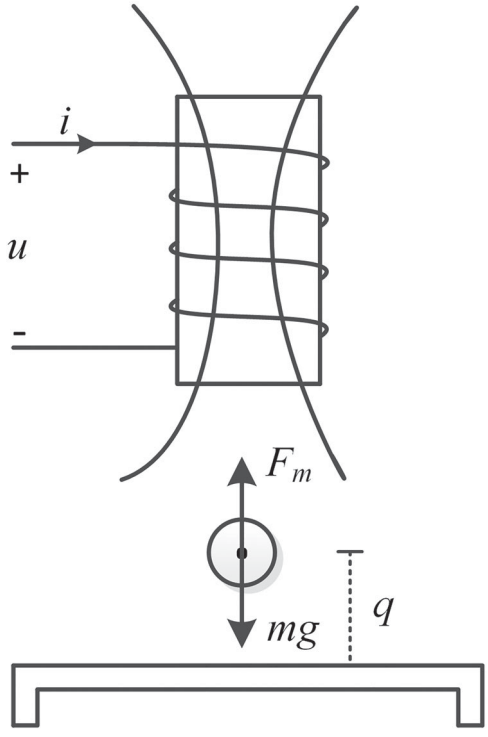

Figure 3. Schematic diagram of a magnetic levitation system.

Table 1. Parameters of the magnetic levitation system (Goodall et al., 2009).

Descriptions	Parameters	Value
Ball mass	M_s	0.5 kg
Nominal air gap	G_o	0.015 m
Nominal current	I_o	1 A
Nominal voltage	V_o	15 V
Coil's resistance	R_c	15 Ω
Coil's inductance	L_c	0.01 H
Number of turns	N_c	200
Pole face area	A_p	0.00002 m^2
Flux density coefficient	K_b	0.033
Magnetic force coefficient	K_f	0.056

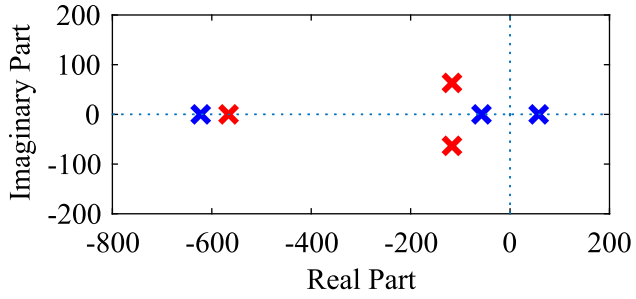

Figure 4. Pole-zero diagram of the MagLev system: open-loop system (the first, fifth and sixth crossmarks from the left), closed-loop system (the second, third and fourth crossmarks from the left).

The physical meanings and values of the MagLev system parameters are given in Table 1 (Goodall et al., 2009). It is easy to prove that the pair $(A,\ B)$ is controllable. The control objective is to regulate the ball to track its desired position q_r.

7.2 Controller design

A stable reference model is designed as follows:

$$A_m = T^{-1}\bar{A}_m T = \begin{bmatrix} 0 & 1 & 0 \\ 3306.63 & 0 & -33.7 \\ 849771 & 10483.9 & -1100 \end{bmatrix}$$

$$B_m = T^{-1}\bar{B}_m = \begin{bmatrix} 0 & 0 & -8000 \end{bmatrix}^{\mathrm{T}}$$

$$C_m = \bar{C}_m T = \begin{bmatrix} 1 & 0 & 0 \end{bmatrix}$$

The error feedback gain is selected as

$$K = \mathbf{0}.$$

Then the complete control law is

$$u = B^{+}\left[(A_m - A)\,x + B_m u_m + \hat{u}_{dmis} - Ke - \hat{u}_d\right]. \qquad (35)$$

It is easy to be checked that the designed matrices A_m and A_c are both Hurwitz. The pole-zero diagram of the MagLev system is displayed in Figure 4, which shows the open-loop system is unstable owing to the right-hand-plane (RHP) pole. As seen, the closed-loop system is dominated by the couple of conjugate poles.

7.3 Simulation results and discussions

Three simulation cases are carried out to verify the effectiveness of the proposed control approach. The controller parameters and filter parameters are given in Tables 2 and 3, respectively. For comparison, the conventional UDE-based control approach in (Ren et al., 2017) is considered.

Table 2. Controller parameters.

Case	Controller $\frac{N'_d(s)}{M'_d(s)}$	k_1	k_2	k_3	k_4
1	$\frac{k_1 s + k_2}{s}$	10	500	–	–
2	$\frac{k_3 s + k_4}{s^2 + \omega_0^2}$	–	–	900	4500
3	$\frac{k_1 s + k_2}{s} + \frac{k_3 s + k_4}{s^2 + \omega_0^2}$	10	500	900	4500

Table 3. Filter parameters.

Case	$G_f(s)$	a	a_1	a_2	ω_0
1	$\frac{a}{s+a}$	20	–	–	–
2	$\frac{a_1 s + a_2 - \omega_0^2}{s^2 + a_1 s + a_2}$	–	$100\omega_0$	$100\omega_0^2$	2π
3	$\frac{a_1 s + a_2 - \omega_0^2}{s^2 + a_1 s + a_2}$	–	$100\omega_0$	$100\omega_0^2$	2π

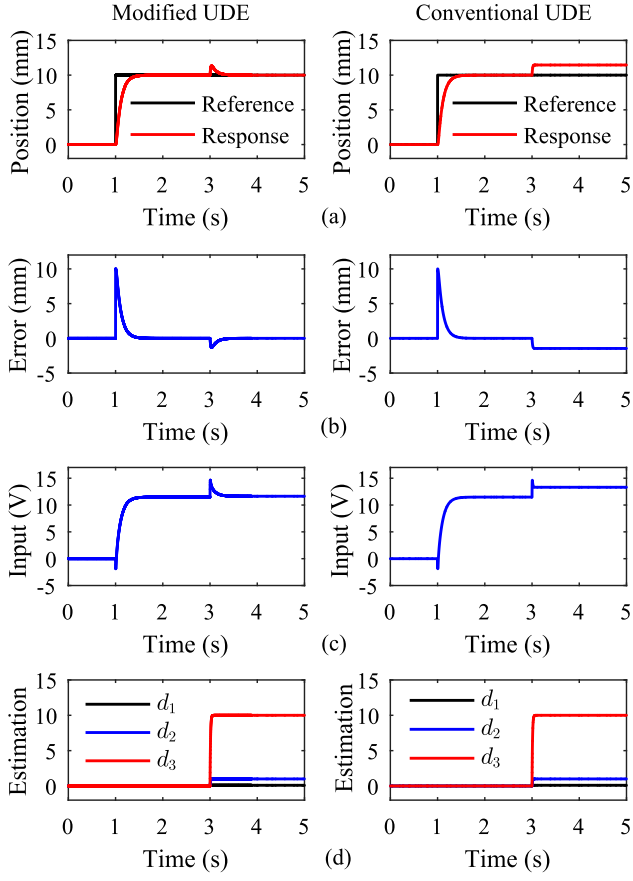

Figure 5. Simulation results of case 1 with the proposed modified UDE-based controller (left column) and the conventional UDE-based controller (Ren et al., 2017) (right column), respectively. (a) Position. (b) Tracking error. (c) Control input. (d) Disturbance estimation.

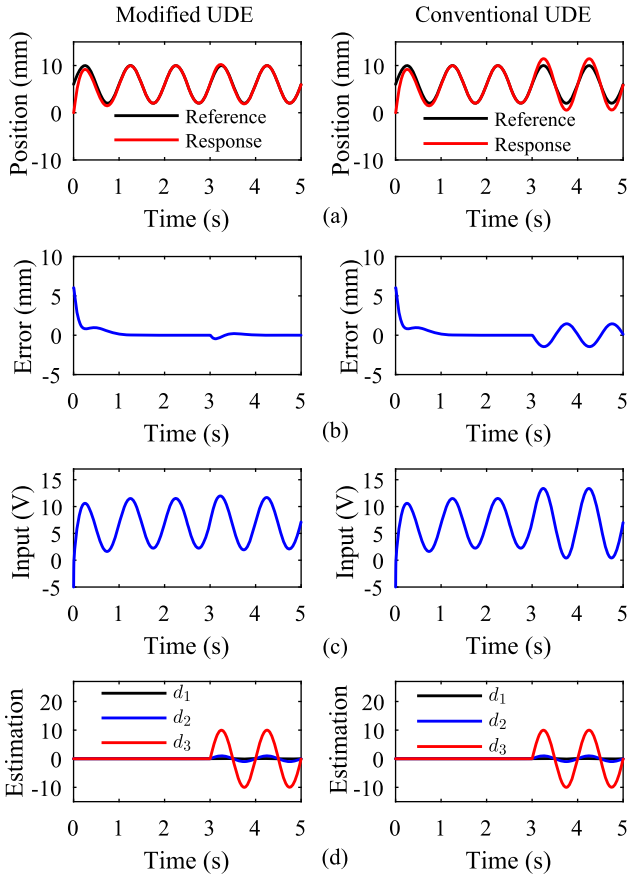

Figure 6. Simulation results of case 2 with the proposed modified UDE-based controller (left column) and the conventional UDE-based controller (Ren et al., 2017) (right column), respectively. (a) Position. (b) Tracking error. (c) Control input. (d) Disturbance estimation.

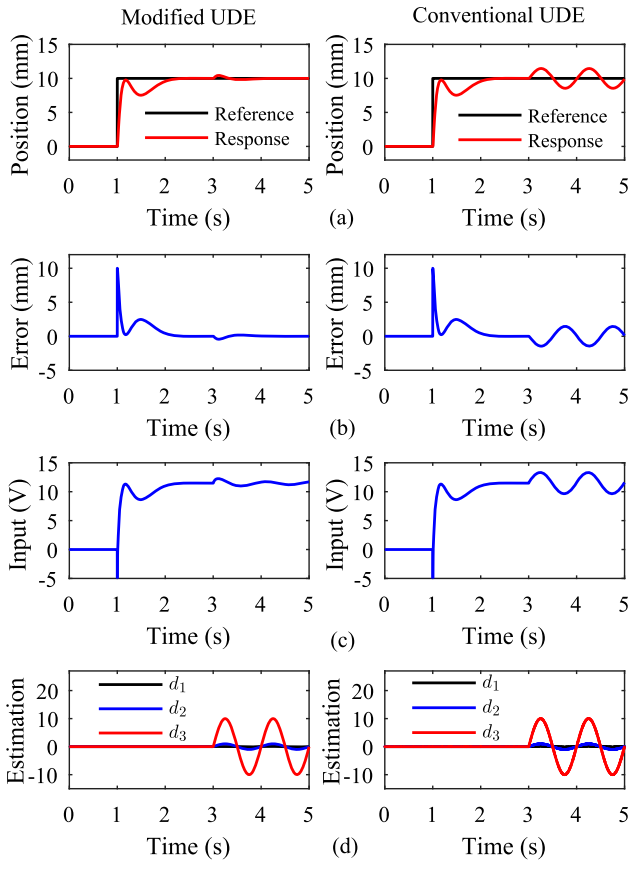

Figure 7. Simulation results of case 3 with the proposed modified UDE-based controller (left column) and the conventional UDE-based controller (Ren et al., 2017) (right column), respectively. (a) Position. (b) Tracking error. (c) Control input. (d) Disturbance estimation.

Case 1: Step signal tracking in the presence of step disturbance

The reference signal q_r steps from zero to 10 mm at time $t = 1$ s and the step disturbance $u_d = [\,0.1\ 1\ 10\,]^{\mathrm{T}}$ is injected into the MagLev system at time $t = 3$ s. It is noticeable that the step disturbance contains both matched component $u_{dm} = [\,0\ 0\ 10\,]^{\mathrm{T}}$ and mismatched component $u_{dmis} = [\,0.1\ 1\ 0\,]^{\mathrm{T}}$. To reject the step disturbance, the controller and filter are designed as the case 1 in Tables 2 and 3, respectively. The initial states of the MagLev system are set to zero. The simulation results with the proposed UDE-based control approach are shown in the left column of Figure 5. It is seen that the proposed control approach achieves excellent tracking performance and good disturbance rejection in the presence of both matched and mismatched disturbances, and the steady tracking error is zero. However, from the right column of Figure 5, it is seen that the conventional UDE-based controller (5) is sensitive to the mismatched disturbance and the steady tracking error is roughly 20% of the reference signal.

Case 2: Sinusoidal signal tracking in the presence of sinusoidal disturbance

The reference position signal is set as $q_r = 6 + 4\sin(\pi t)$ mm and the sinusoidal disturbance $u_d = [\,0.1\ 1\ 10\,]^{\mathrm{T}}\sin(2\pi t)$ V is injected into the MagLev system at time $t = 3$ s. To reject the sinusoidal disturbance, the controller and filter are designed as the case 2 in Tables 2 and 3, respectively. From Figure 6, it is seen that the proposed UDE-based control approach achieves perfect tracking with the sinusoidal reference signal and the steady tracking error converges to zero after 0.5 s transient time. Nevertheless, the conventional UDE-based controller (5) almost loses its tracking ability owing to the large oscillation on tracking error.

Case 3: Step signal tracking in the presence of sinusoidal disturbance

The reference signal q_r steps from zero to 10 mm at time $t = 1$ s and the sinusoidal disturbance $u_d = [\,0.1\ 1\ 10\,]^{\mathrm{T}}\sin(2\pi t)$ is injected into the MagLev system at time $t = 3$ s. To reject the sinusoidal disturbance, the controller and filter are designed as the case 3 in Tables 2 and 3, respectively. From Figure 7, it is observed that the proposed UDE-based control approach presents good tracking ability and disturbance rejection. The tracking error converges to zero after a short transient time. But for the the conventional UDE-based controller (5), it is seen that the sinusoidal disturbance brings to large oscillation on the position tracking.

8. Conclusions

In this paper, an improved UDE-based robust control approach is proposed to achieve asymptotic tracking for a general type system with mismatched uncertainties. Based on the UDE and

internal model principle, the effects of both matched and mismatched uncertainties could be completely eliminated. Moreover, the proposed control approach retains the two-degree-of-freedom nature, which achieves the decoupling of reference tracking and disturbance rejection in the frequency domain. Compared with the previous studies, the proposed approach does not require integrations with other complex control methods, and the upper bounds of uncertainties are unnecessary for the robust controller design. In the future, the implementations and applications of the proposed approach in power converters or permanent magnet synchronous machines will be considered to test its feasibility and control performance. For practical disturbances and uncertainties, we may need to test or estimate their frequency information (bandwidth) so that appropriate UDE filter could be selected. Besides, to overcome its drawback of full states measurement, design issues of the UDE-based output-feedback controller will be investigated by integrating with the state observers.

Disclosure statement

No potential conflict of interest was reported by the authors.

Funding

This work was supported by National Natural Science Foundation of China [grant number 61533013] and Natural Science Foundation of Shanghai [grant number 17ZR1414200].

References

Aharon, I., Shmilovitz, D., & Kuperman, A. (2018). Uncertainty and disturbance estimator-based controllers design under finite control bandwidth constraint. *IEEE Transactions on Industrial Electronics*, *65*(2), 1439–1449.

An, H., Liu, J., Wang, C., & Wu, L. (2016). Disturbance observer-based antiwindup control for air-breathing hypersonic vehicles. *IEEE Transactions on Industrial Electronics*, *63*, 3038–3049.

Andrade-Da Silva, J. M., Edwards, C., & Spurgeon, S. K. (2009). Sliding mode output-feedback control based on LMIs for plants with mismatched uncertainties. *IEEE Transactions on Industrial Electronics*, *56*, 3675–3683.

Arefi, M. M., Jahed-Motlagh, M. R., & Karimi, H. R. (2015). Adaptive neural stabilizing controller for a class of mismatched uncertain nonlinear systems by state and output feedback. *IEEE Transactions on Cybernetics*, *45*, 1587–1596.

Arefi, M. M., & Jahed-Motlagh, M. (2012). Adaptive robust stabilization of a class of uncertain non-linear systems with mismatched time-varying parameters. *Proceedings of the Institution of Mechanical Engineers, Part I: Journal of Systems and Control Engineering*, *226*, 204–214.

Cao, W. J., & Xu, J. X. (2004). Nonlinear integral-type sliding surface for both matched and unmatched uncertain systems. *IEEE Transactions on Automatic Control*, *49*, 1355–1360.

Cervera, A., & Peretz, M. M. (2018). Modelling and control of magnetic actuation systems based on sensorless displacement information. *IEEE Transactions on Industrial Electronics*, *66*(6), 4849–4859.

Dai, J., Ren, B., & Zhong, Q. C. (2018). Uncertainty and disturbance estimator-based backstepping control for nonlinear systems with mismatched uncertainties and disturbances. *Journal of Dynamic Systems, Measurement and Control*, *140*(12), 121005–121005-11.

Dai, J., Ren, B., & Zhong, Q. C (2016). UDE-based dynamic surface control for strict-feedback systems with mismatched disturbances. *Proceedings of 2016 American Control Conference* (pp. 4743–4748).

Francis, B., & Wonham, W. M. (1976). The internal model principle of control theory. *Automatica*, *12*, 457–465.

Ginoya, D., Shendge, P., & Phadke, S. (2014). Sliding mode control for mismatched uncertain systems using an extended disturbance observer. *IEEE Transactions on Industrial Electronics*, *61*, 1983–1992.

Goodall, R., Michail, K., Whidborne, J., & Zolotas, A (2009). *Optimised configuration of sensing elements for control and fault tolerance applied to an electro-magnetic suspension*. PhD Thesis, Loughborough University, UK.

Guo, B. Z., & Wu, Z. H. (2017). Output tracking for a class of nonlinear systems with mismatched uncertainties by active disturbance rejection control. *Systems and Control Letters*, *100*, 21–31.

Hu, Q. (2007). Robust integral variable structure controller and pulse-width pulse-frequency modulated input shaper design for flexible spacecraft with mismatched uncertainty/disturbance. *ISA Transactions*, *46*, 505–518.

Huang, A. C., & Chen, Y. C. (2004). Adaptive multiple-surface sliding control for non-autonomous systems with mismatched uncertainties. *Automatica*, *40*, 1939–1945.

Khalil, H. K. (1996). *Noninear systems*. Upper Saddle River, NJ: Prentice-Hall.

Li, S., Yang, J., Chen, W. H., & Chen, X. (2012). Generalized extended state observer based control for systems with mismatched uncertainties. *IEEE Transactions on Industrial Electronics*, *59*, 4792–4802.

Liu, H., & Li, S. (2012). Speed control for PMSM servo system using predictive functional control and extended state observer. *IEEE Transactions on Industrial Electronics*, *59*, 1171–1183.

Liu, C., Liu, G., & Fang, J. (2017). Feedback linearization and extended state observer-based control for rotor- AMBs system with mismatched uncertainties. *IEEE Transactions on Industrial Electronics*, *64*, 1313–1322.

Londhe, P., Dhadekar, D. D., Patre, B., & Waghmare, L. (2017). Uncertainty and disturbance estimator based sliding mode control of an autonomous underwater vehicle. *International Journal of Dynamics and Control*, *5*, 1122–1138.

Marino, R., & Tomei, P. (2014). Robust adaptive compensation of periodic disturbances with unknown frequency. *IEEE Transactions on Automatic Control*, *59*, 2760–2765.

Ren, B., Zhong, Q. C., & Chen, J. (2015). Robust control for a class of nonaffine nonlinear systems based on the uncertainty and disturbance estimator. *IEEE Transactions on Industrial Electronics*, *62*, 5881–5888.

Ren, B., Zhong, Q. C., & Dai, J. (2017). Asymptotic reference tracking and disturbance rejection of UDE-based robust control. *IEEE Transactions on Industrial Electronics*, *64*, 3166–3176.

Sanz, R., Garcia, P., Albertos, P., & Zhong, Q. C. (2017). Robust controller design for inputdelayed systems using predictive feedback and an uncertainty estimator. *International Journal of Robust and Nonlinear Control*, *27*, 1826–1840.

Sun, L., Li, D., Zhong, Q. C., & Lee, K. Y. (2016). Control of a class of industrial processes with time delay based on a modified uncertainty and disturbance estimator. *IEEE Transactions on Industrial Electronics*, *63*, 7018–7028.

Wang, J., Li, S., Yang, J., Wu, B., & Li, Q. (2015). Extended state observer-based sliding mode control for PWM-based DC-DC buck power converter systems with mismatched disturbances. *IET Control Theory and Applications*, *9*, 579–586.

Wang, J., Li, S., Yang, J., Wu, B., & Li, Q. (2016). Finite-time disturbance observer based nonsingular terminal sliding-mode control for pulse width modulation based DC-DC buck converters with mismatched load disturbances. *IET Power Electronics*, *9*, 1995–2002.

Yang, J., Li, S., & Yu, X. (2013). Slidingmode control for systems with mismatched uncertainties via a disturbance observer. *IEEE Transactions on Industrial Electronics*, *60*, 160–169.

Yang, J., Zolotas, A., Chen, W. H., Michail, K., & Li, S. (2011). Robust control of nonlinear maglev suspension system with mismatched uncertainties via DOBC approach. *ISA Transactions*, *50*, 389–396.

Zhai, D., An, L., Dong, J., & Zhang, Q. (2017). Robust adaptive fuzzy control of a class of uncertain nonlinear systems with unstable dynamics and mismatched disturbances. *IEEE Transactions on Cybernetics*, *99*, 1–11.

Zhang, J., Shi, P., & Xia, Y. (2010). Robust adaptive sliding-mode control for fuzzy systems with mismatched uncertainties. *IEEE Transactions on Fuzzy Systems*, *18*, 700–711.

Zhao, Z. L., & Guo, B. Z. (2018). A novel extended state observer for output tracking of MIMO systems with mismatched uncertainty. *IEEE Transactions on Automatic Control*, *63*, 211–218.

Zhong, Q. C., Kuperman, A., & Stobart, R. (2011). Design of UDE-based controllers from their two-degree-of-freedom nature. *International Journal of Robust and Nonlinear Control*, *21*, 1994–2008.

Zhong, Q. C., & Rees, D. (2004). Control of uncertain LTI systems based on an uncertainty and disturbance estimator. *Journal of Dynamic Systems, Measurement and Control*, *126*, 905–910.

Zhu, Y., & Zhu, S. (2014). Adaptive sliding mode control based on uncertainty and disturbance estimator. *Mathematical Problems in Engineering*, *2014*, 1–10.